2017 International Nuclear Atlantic Conference - INAC 2017
Belo Horizonte, MG, Brazil, October 22-27, 2017
ASSOCIAÇÃO BRASILEIRA DE ENERGIA NUCLEAR – ABEN

Agência Brasileira do ISBN
ISBN 978-85-99141-07-6
9 788599 141076

PRESERVATION OF PHOTOGRAPHIC AND CINEMATOGRAPHIC FILMS BY GAMMA RADIATION- PRELIMINARY ANALYSES

Maria Luiza E. Nagai[1], Paulo S. Santos[1], Larissa Otubo[1], Maria José A. Oliveira[1] and Pablo A. S. Vasquez[1]

[1] Instituto de Pesquisas Energéticas e Nucleares (IPEN / CNEN - SP)
Av. Professor Lineu Prestes 2242
05508-000 São Paulo, SP
malunagai@usp.br
pavsalva@ipen.br

ABSTRACT

Brazilian weather conditions affect directly tangible materials causing deterioration notably getting worse by insects and fungi attack. In this sense, gamma radiation provided from the cobalt-60 is an excellent alternative tool to the traditional preservation process mainly because it has biocidal action. Radiation processing using gamma radiation for cultural heritage materials for disinfection has been widely used around the world in the last decades. Many cultural heritage objects especially made on paper and wood were studied in scientific publications aiming mechanical, physical and chemical properties changes. Over the last fifteen years, the Multipurpose Gamma Irradiation Facility of the Nuclear and Energy Research Institute located inside the Sao Paulo University campus has been irradiated many collections of archived materials, books, paintings and furniture. Adequate storage of photographic and cinematographic materials is a challenge for conservators from preservation institutions. Contamination by fungi is one of leading causes of problem in photographic and cinematographic collections. Several Sao Paulo University libraries have been affected by fungi in their photographic and cinematographic collections making it impossible to research on these materials either manipulate them for health and safety reasons. In this work are presented preliminary results of effects of the ionizing radiation in photographic and cinematographic films. Selected film samples made on cellulose acetate were prepared and characterized by FTIR-ATR spectroscopy. Samples were irradiated by gamma rays with absorbed dose between 2 kGy and 50 kGy. Irradiated samples were analyzed by UV-VIS spectroscopy and electron microscopy techniques. Results shown that disinfection by gamma radiation can be achieved safely applying the disinfection dose between 6 kGy to 15 kGy with no significant change or modification of main properties of the constitutive materials.

1. INTRODUCTION

Safeguarding photographic and cinematographic films collections has been a challenge to conservators due to materials nature used as film support and the storage conditions with high temperatures and humidity. Majority of black-and-white photographic and cinematographic films on libraries, museums and historical archives collections are made on cellulose acetate (CA) base. CA is a polymer that has been used nowadays as membrane filters, yarn for textile industry, anti-fog goggles, dosimeters, optical film for LCD technology, semipermeable film for pharmaceutical products and also was widely used as a photographic film support in the mid-1920s until 1990s. CA is a semisynthetic polymer of the cellulose esters produced by a thermoplastic process. CA properties include toughness, clarity, low permeability, good chemical resistance and flexibility. CA base is obtained from a blend made of cotton linters, acetic acid, acetic anhydride and sulfuric acid as a catalyst (Figure 1). Often plasticizers like triphenyl phosphate (TPP), for instance, are added to improve flexibility, toughness and

moisture resistance. Layers are applied in the case of black-and-white photographic and cinematographic films namely an adhesive layer to adhere the gelatin emulsion to the CA base, an anti-halation layer to protect the film and other surface coatings to provide static protection (Figure 2). The physical and chemical stability of CA are affected by temperature and humidity. It was observed CA base materials stored under hot and humid conditions presented physical and chemical degradation characterized by the emission of acetic acid known as "vinegar syndrome" due deacetylation process and breakdown of the CA [1, 2]. Furthermore fungi attacks have been associated with storage at high temperature and humidity. Gelatin emulsion and CA base from films are the food source for fungus growth. A leading cause of deterioration of photographic and cinematographic films by microbiological agents is the fungi attack. Thus, researches on new technologies have been developed for the treatment disinfection in photographic and cinematographic materials.

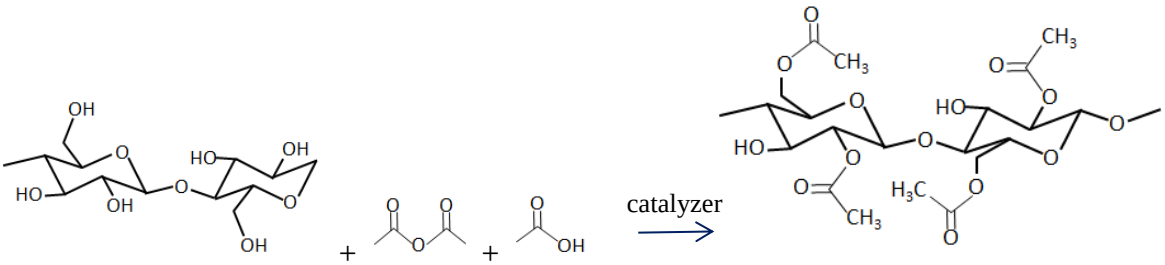

Figure 1: Manufacturing process of cellulose acetate.

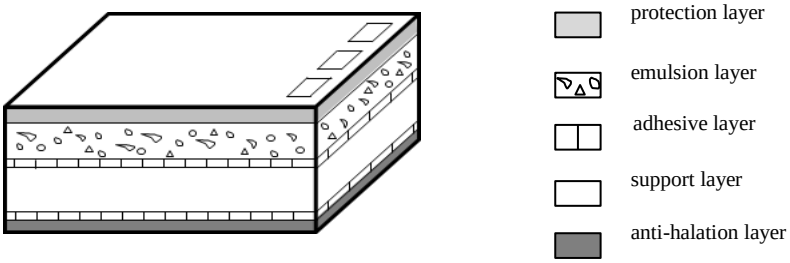

Figure 2: Layer's scheme of a photographic and cinematographic film

Radiation processing technology currently is widely applied around the world. Over 250 gamma irradiation facilities are in operation for a variety of purposes in 55 countries; 140 of these plants are located in Europe and North America [3]. Products sterilized by gamma radiation have wide range of applications among them medical devices and medical supplies such as syringes, surgical gloves, catheters, masks, adhesive bandages, packaging, etc. Food irradiation as well has been applied, reducing or eliminating disease-causing germs and increasing the quality control. Other materials including artificial joints, animal feed, raw materials for pharmaceuticals and cosmetics, and even wine corks are gamma processed [4]. The last years were enhanced and intensified gamma sterilization treatments of human tissues for transplantation including bones, skin, amniotic membranes, tendons, and cartilage. The same happened with cultural heritage materials as books, parchments, canvas, paintings,

textiles, leather, sculptures, furniture, photographs, cinematographic films, etc. where gamma radiation has helped to eliminate insects and fungi. Several studies have been conducted to determine the ideal dose to eliminate fungi contamination in cultural heritage materials and it has been found that doses between 6kGy and 10kGy are effective to fade away the microbiological contamination in cellulose materials [5, 6, 15]. A limit around 12kGy was recommended to not affect the physical and chemical properties [7,15]. Thereby, the breakthrough of researches radiation processing by gamma rays to preserve the cultural heritage has been promising in the conservation science. In this study, samples were characterized by FTIR-ATR spectroscopy to know their compositions. Electron microscopy was used to analyze and characterize the surface morphology of non-irradiated and the effective disinfected (10kGy) films samples. Non-irradiated and irradiated samples between 2kGy and 50kGy were evaluated by UV-VIS absorption to determine the effective dose to eliminate the fungi contamination and preserve the material properties of the photographic and cinematographic films.

2. MATERIALS AND EXPERIMENTAL

2.1. Films samples selection and preparation

For this study, two black-and-white photographic and cinematographic films samples were selected from USP libraries. Table 1 shows the main properties of the selected materials. Several samples were cut into small pieces in order to fit in different equipment samplers.

Table 1: Films samples properties

Sample No.	Film type	Thickness (mm)
N5	Negative – Photographic	0.242±0.001
F1	Cinematographic	0.124±0.001

2.2. Irradiation by gamma rays from cobalt-60 sources

The samples were irradiated at the Multipurpose Gamma Irradiation Facility of the Nuclear and Energy Research Institute – IPEN/CNEN located inside the University of São Paulo campus. This facility is a panoramic wet source storage compact irradiator (IAEA - Category IV) that means, when it not in use, the radioactive sources are stored and fully shielded in a pool of 7 meters depth deionized water [8, 9]. The facility uses cobalt-60 source pencils where the radiative material was encapsulated in corrosion resistant stainless steel such that gamma radiation can come through but not the radioactive material itself, eliminating the risk of contamination. The installed activity of the facility is around 11.1PBq (300kCi) [11,12]. The source pencils (48 units) were loaded into predetermined positions in source modules and distributing these modules over the source racks. The racks are the structures that house all the source pencils enabling the movement of the source system from the bottom of the pool to the irradiation chamber level [10].

Samples were irradiated by gamma rays with following absorbed dose 2, 6, 10, 15, 20, 25 and 50 kGy. Dose rate was 5-6kGy/h. The absorbed dose, *D*, is the amount of energy absorbed per unit mass of irradiated matter at a point in the region of interest. It is defined as the mean energy, $d\bar{\varepsilon}$, imparted by ionizing radiation to the matter in a volume element divided by the mass, *dm*, of that volume element [11]:

$$D = \frac{d\bar{\varepsilon}}{dm} \quad (1)$$

The SI derived unit of absorbed dose is the gray (Gy), which replaced the earlier unit of absorbed dose, the rad, 1 Gy = 1 J/kg = 100 rad.
The PMMA-Harwell dosimetry system was used to calculate the absorbed dose in the irradiated samples [11,12].

2.3. Attenuated total reflection Fourier-transform infrared spectroscopy (FTIR-ATR)

Samples were analyzed by FTIR-ATR to characterization organic compounds of the materials. Spectra were collected using a Thermo Scientific Nicolet FTIR-ATR 6700 with range from 4000 to 400 wavenumber (cm^{-1}).

2.4. Ultraviolet-Visible Spectroscopy (UV-VIS)

Changes in color of the gamma irradiated materials can occur due to the excitation of the electrons depending of the absorbed dose. For this reason, the UV-visible spectroscopy was chosen to ensure that the effective disinfection dose do not induce secondary effects in the constitutive materials also because the films have transparent characteristics. Absorption spectra were carried out using Shimadzu UV-1601PC model UV-Visible spectrophotometer with scan range of 190 to 1100 nm. The measured absorbance was normalized to the thickness of the films samples to find specific absorbance. Samples thickness were measured three times with a digital micrometer Mitotuyo code nº 156-101, Mexico, and was calculated the median values of each sample.

2.5. Field-emission Gun Scanning Electron Microscopy (FEGSEM) and Energy Dispersive Spectroscopy (EDS)

Scanning electron microscopy was used to analyze and characterize the non-irradiated (0kGy) and the effective disinfected (10kGy) films samples. Preliminary observations shown two regions inside N5 sample, a darkest area that received the most light exposure and a clearest area that received no light. In the darkest area the silver halide molecules was converted to metallic silver and on clearest area the silver halide it was not converted. Then for microscopy purposes it was divided in N5-w (white) for clearest area and N5-b (black) for darkest area. Surface topography and elemental analysis of the films were analyzed by scanning electron microscopy (FEGSEM), using a Jeol JSM-6701F electron microscope with a field emission gun operating at 1kV and 6kV with a coupled Thermo EDS detector. A piece of each sample was cut and fixed with a double sided conducting carbon tape. The images

were taken with the “raw” samples at an accelerating voltage of 1kV, but for EDS analysis, the samples were previously coated with carbon to avoid damage using 6kV of accelerating voltage. For semi-quantification of elements, it was chosen a general scan for the elements distributions of the samples and a single point individual analyses, which means selecting many points to reach the composition of a selected region of the micrographs [13].

3. RESULTS AND DISCUSSION

3.1. FTIR-ATR spectroscopy analysis

The infrared spectra of two samples showed coincident peaks of cellulose acetate, gelatin and triphenyl phosphate (Fig. 3). Spectra were accented by the C–H stretching region between 3000 cm^{-1} and 2800 cm^{-1}, carbon double bond region between 1800 cm^{-1} and 1500 cm^{-1} and the fingerprint region (incorporating the amide region and C–H deformation region) between 1500 cm^{-1} and 500 cm^{-1}. The C–H stretching region has two prominent peaks at approximately 2969 cm^{-1} (CH_3 asymmetric stretch) and 2865 cm^{-1} (CH_2 asymmetric stretch). Carbonyl stretching (C=O) region has one peak at approximately 1726 cm^{-1}. The amide II region has one peak at approx. 1531 cm^{-1}. The C–H deformation region has one peak at approx. 1373 cm^{-1} (asymmetric deformation of CH_3). Fingerprint region has strong peaks between approximately 1074 cm^{-1} and 600 cm^{-1}. The exact peak positions and probably assignments for two spectra are given in Table 2.

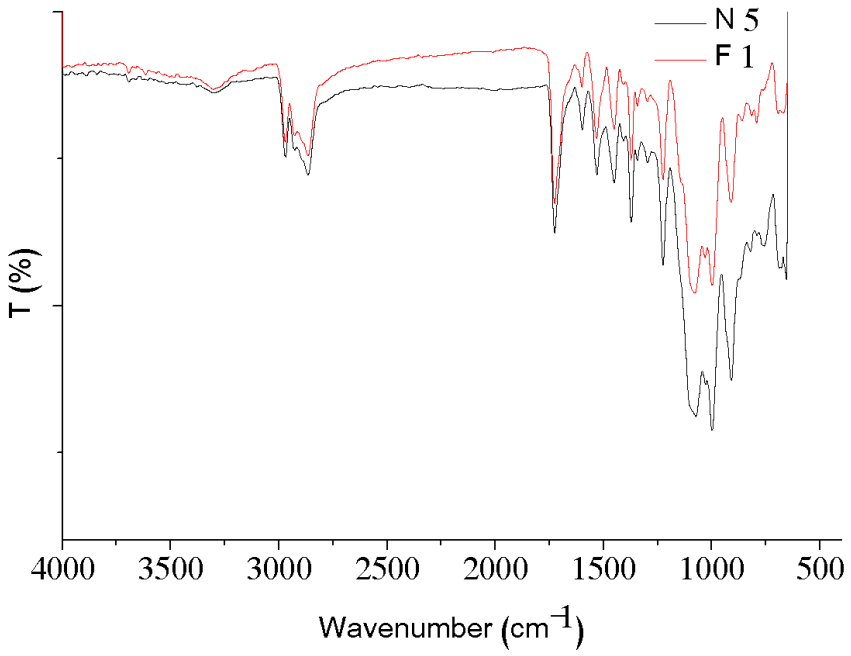

Figure 3: FTIR spectra (4000-500 cm^{-1}) for samples N5 and F1.

Table 2: FTIR absorption frequencies results and sample characterization

Wavenumber (cm^{-1})	**Functional class**	**Assignment**	**Origin**
2969	Alkanes	CH_3 asymmetric stretch	CA
2865	Alkanes	CH_2 asymmetric stretch	Gelatin
1726	Aldehydes	C=O saturated aldehyde	CA
1598	Amines	NH_2 scissoring (1°-amines)	Gelatin
1531	Amine II	N-H bending absorption	Gelatin
1452	Aldehydes	CH_2 bending	Gelatin
1373	Alkane	CH_3 deformation	CA
1224	Carboxylic Acid	O-C	Gelatin, CA
1074	Alcohols & Phenol	C-O	Gelatin, CA, TPP
998	Phosphorous	P-OR esters	TPP
910	Phosphorous	P-OR esters	TPP
759	Amine II	N-H bending absorption (wag)	Gelatin
655	Amine II	N-H bending absorption (wag)	Gelatin

3.2. UV-VIS spectroscopy analysis

Figure 4 shows the UV-visible absorption spectra of samples N5 and F1 irradiated with different gamma rays irradiation doses. Both samples were colorless and opaque films. Spectra N5 sample presented an increase of the absorbance intensity after the range of 400nm without evidence of any specific peak. UV-visible spectra of F1 sample showed a weak peak between 450-300nm and increase absorbance intensity after approximately 300nm. UV-visible absorption spectra of negative and cinematographic film samples did not present detectable modifications produced by gamma rays doses from 0kGy until 50kGy. The changes of the spectra of irradiated and non-irradiated samples were statistically no significant.

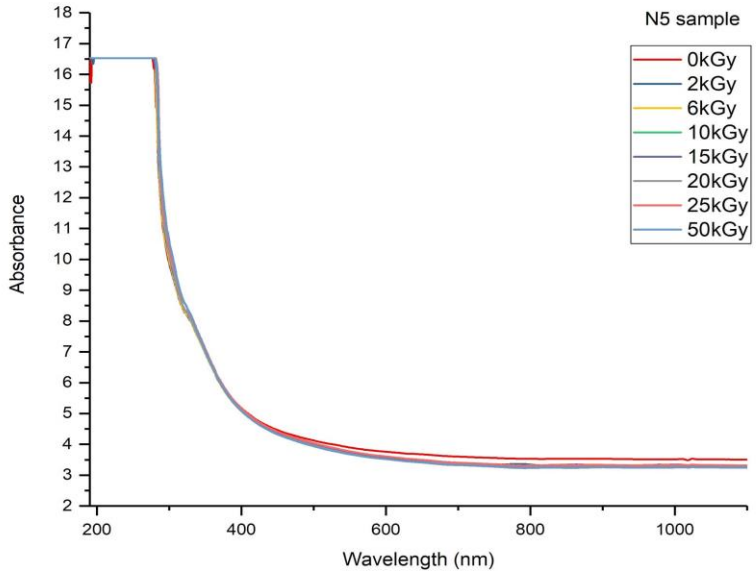

(a)

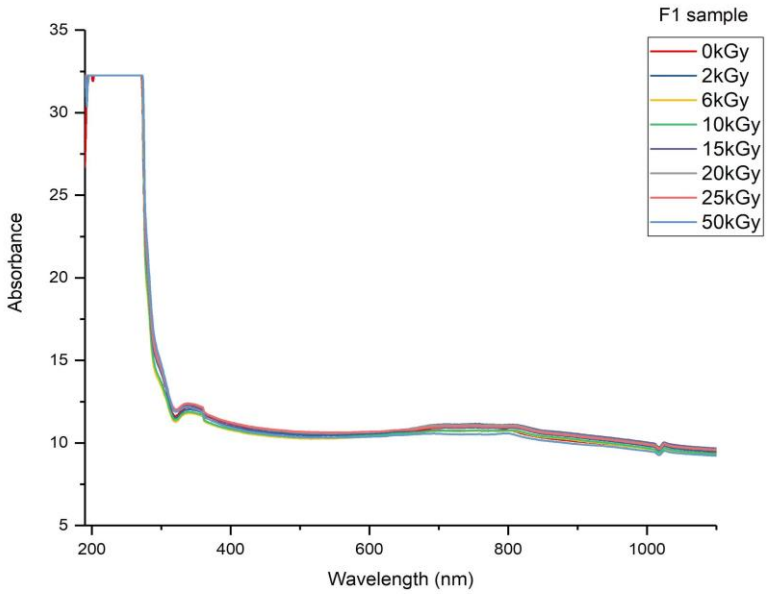

(b)

Figure 4: UV-VIS absorption spectra samples N5 (a) and F1 (b).

3.3. FEGSEM microscopy analyses

No effect of the irradiation on the structure of the samples can be observed on the FEGSEM images of non-irradiated and gamma irradiated samples as shown in Figure 5. The images show different morphologies for F1 and N5 films: the latter is covered by very small particles observed as bright dots on the surface of the films, both white and black areas. In addition, elemental analysis were carried out with EDS coupled to the SEM.

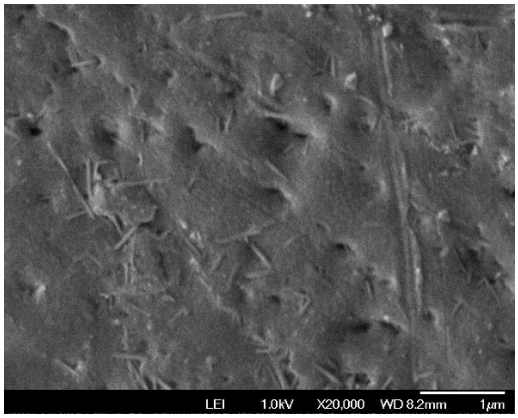

0kGy

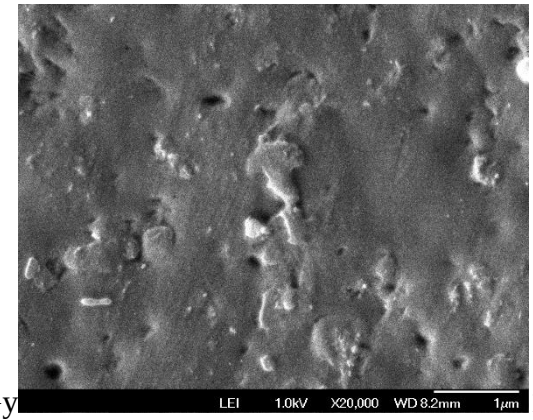

10kGy

(a)

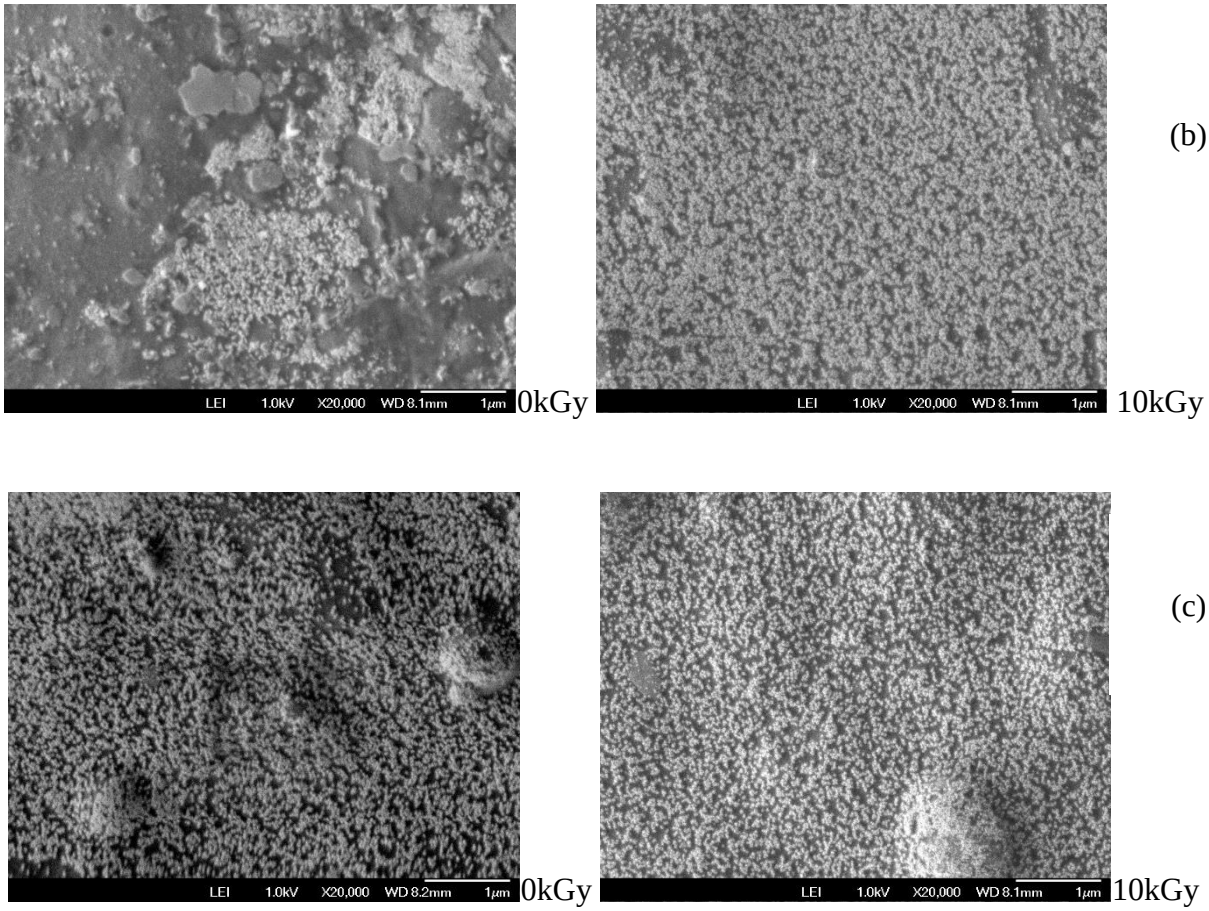

Figure 5: FEGSEM micrographs of the non–irradiated (0kGy) and irradiated samples (10kGy): (a) F1, (b) N5-w, and (c) N5-b.

3.4. FEGSEM-EDS spectroscopy analyses

a. Elemental distribution analyses

FEGSEM-EDS was used to study the homogeneity and the elemental compositions of the samples. The results are shown in Figure 6, 7, 8, 9 and Table 3. Figures 6, 7 and 8 depict the mapping of elemental distribution on the sample surface, shown by different color images, according to each element. Figure 9 shows the EDS spectra of the films, and the results are on table 3, to facilitate comparison of the results. All samples show carbon and oxygen as majority elements due to the organic compounds of film materials such as gelatin and cellulose acetate. Furthermore, coating samples with carbon (during preparation for microscopy analysis) enhances the carbon peak of the EDS spectrum (Figure 9). Silver are present in all samples with a good distribution in the materials. Phosphorus from triphenyl phosphate plasticizer can be observed in sample F1 (Figure 9). Presence of sulfur may occur because of the thiosulfate from fixing solution in the reversal process black and white films. Aluminum can be attributed to the sample-holder material. Molybdenum and silicon can be attributed to external contaminants. The presence of chloride in sample N5-b may be derived

from the flame retardant additive used in the films. The composition of these elements in both of samples was similar.

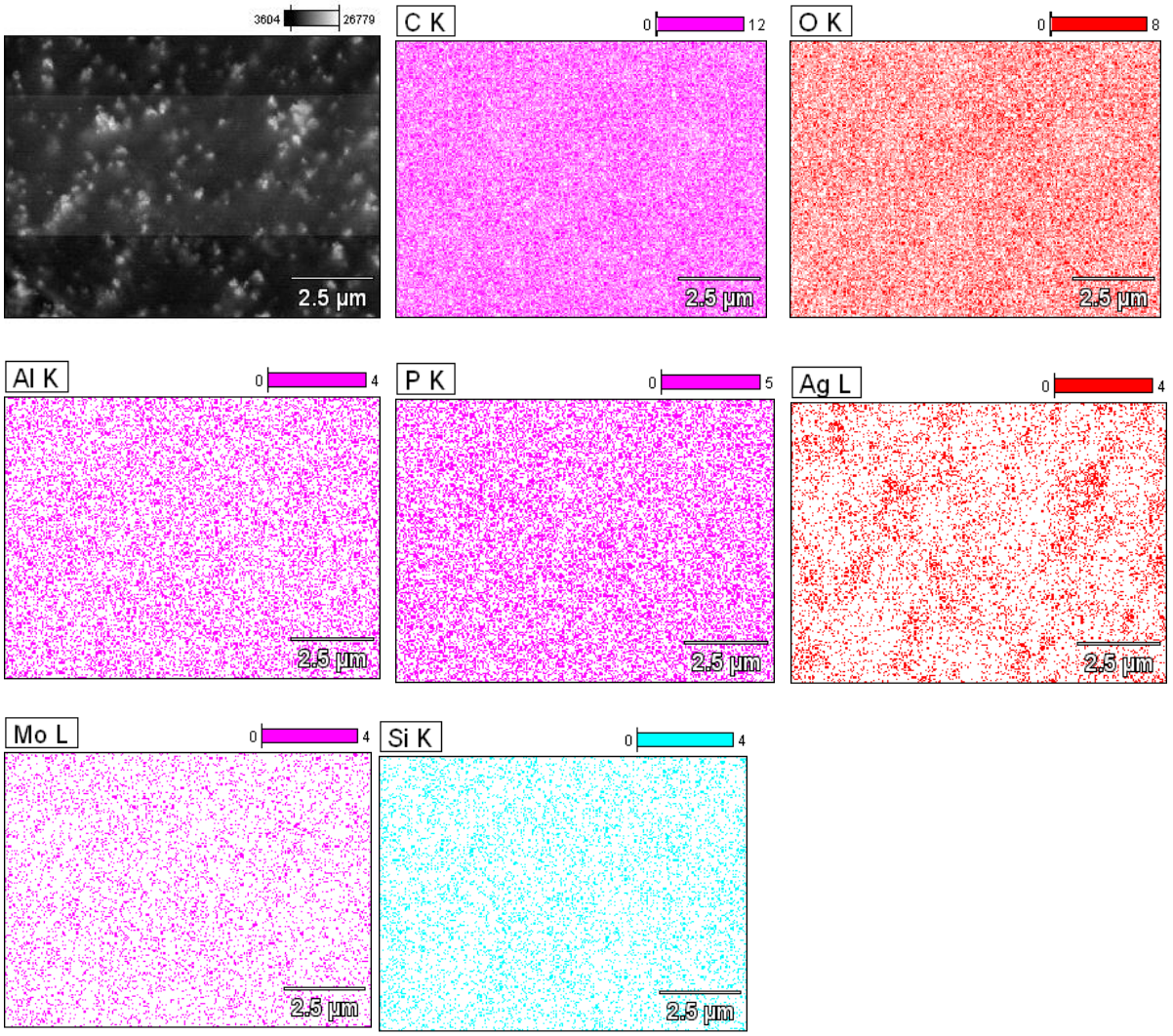

Figure 6: FEGSEM-EDS mapping of the elements distribution analysis of the non–irradiated F1 sample.

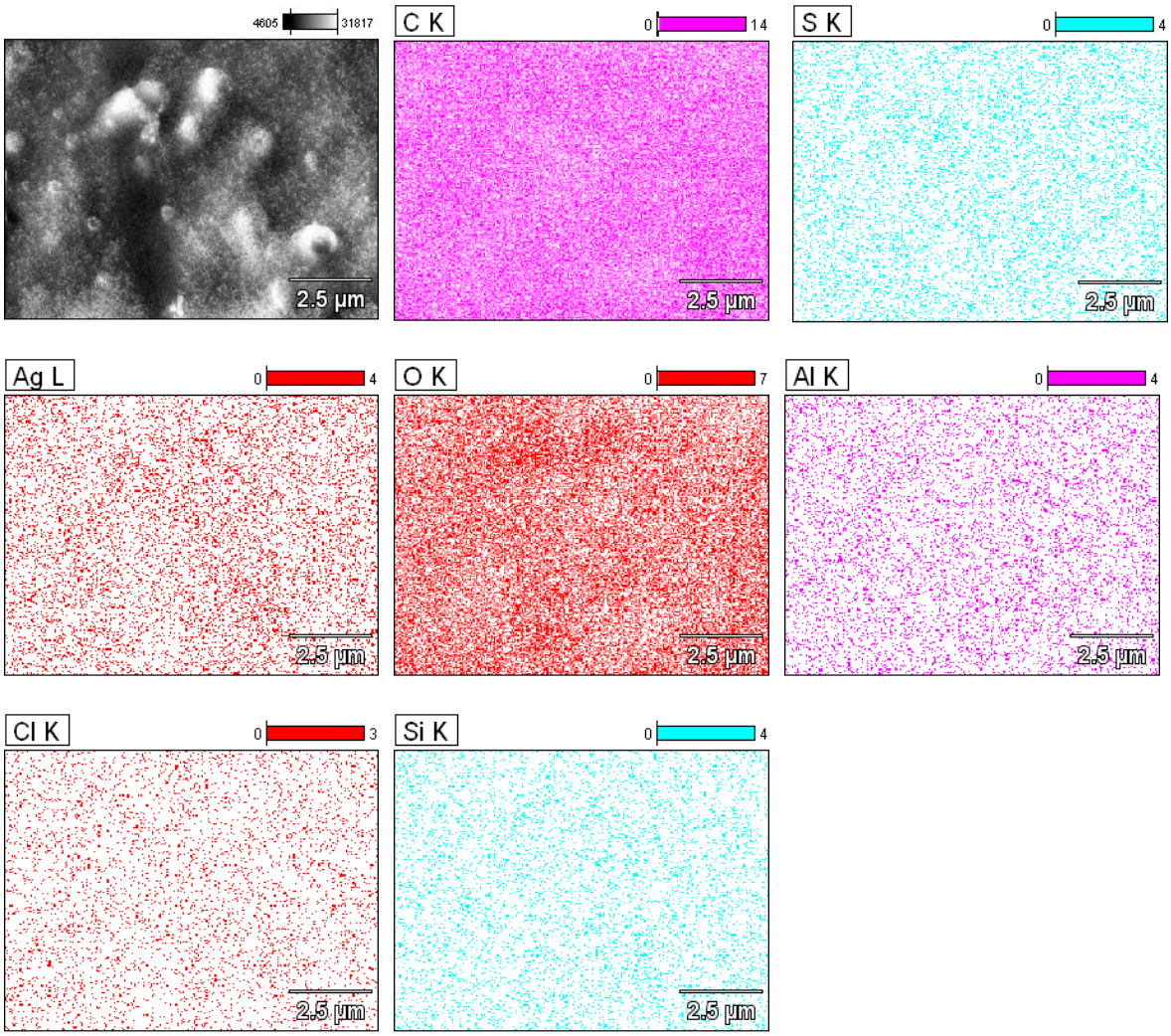

Figure 7: FEGSEM-EDS elements distribution analysis of the non–irradiated N5-w sample.

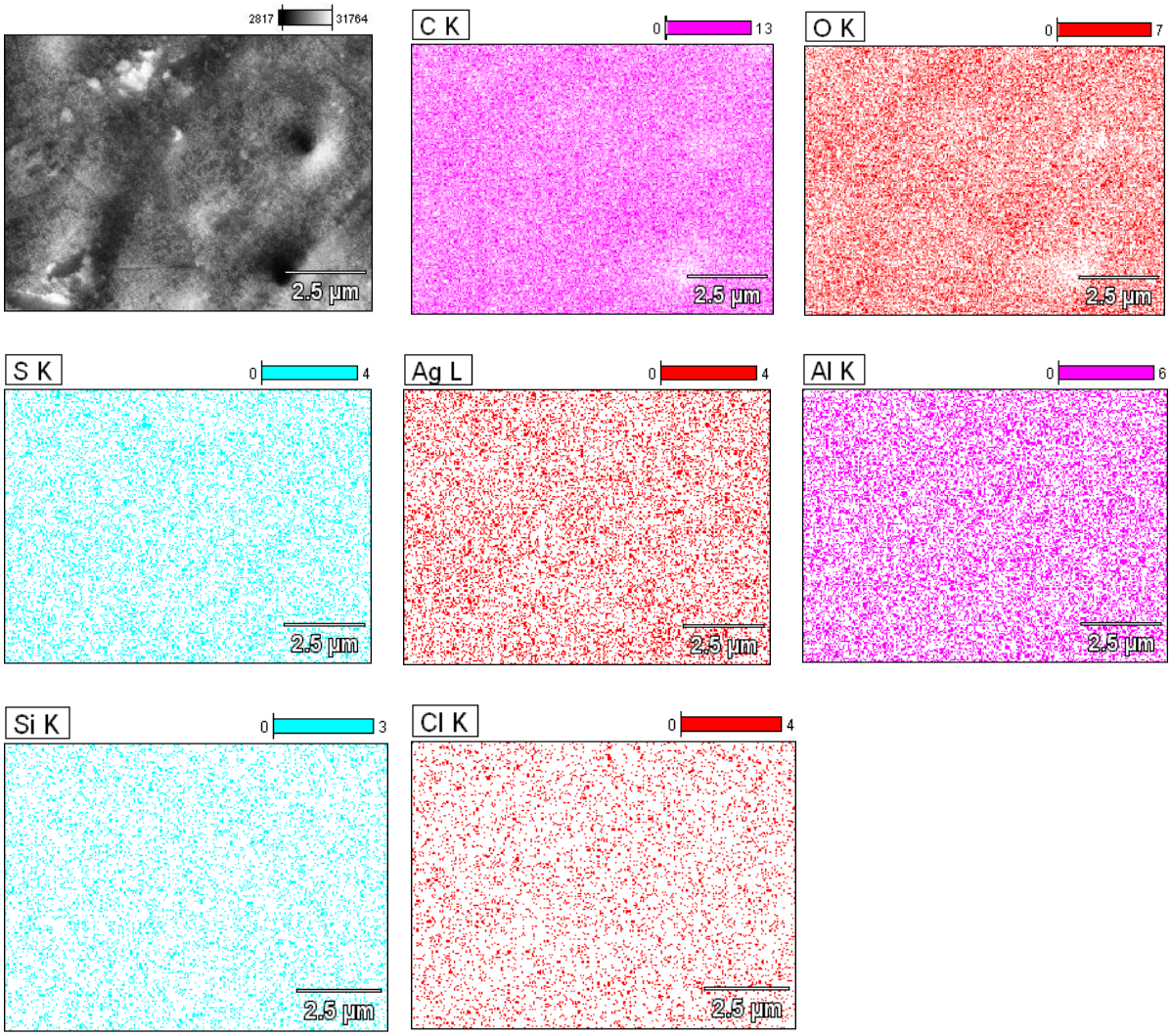

Figure 8: FEGSEM-EDS elements distribution analysis of the non–irradiated N5-b sample.

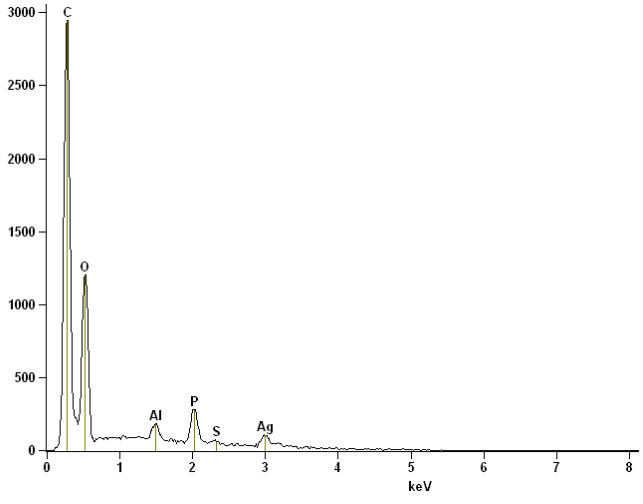

(a)

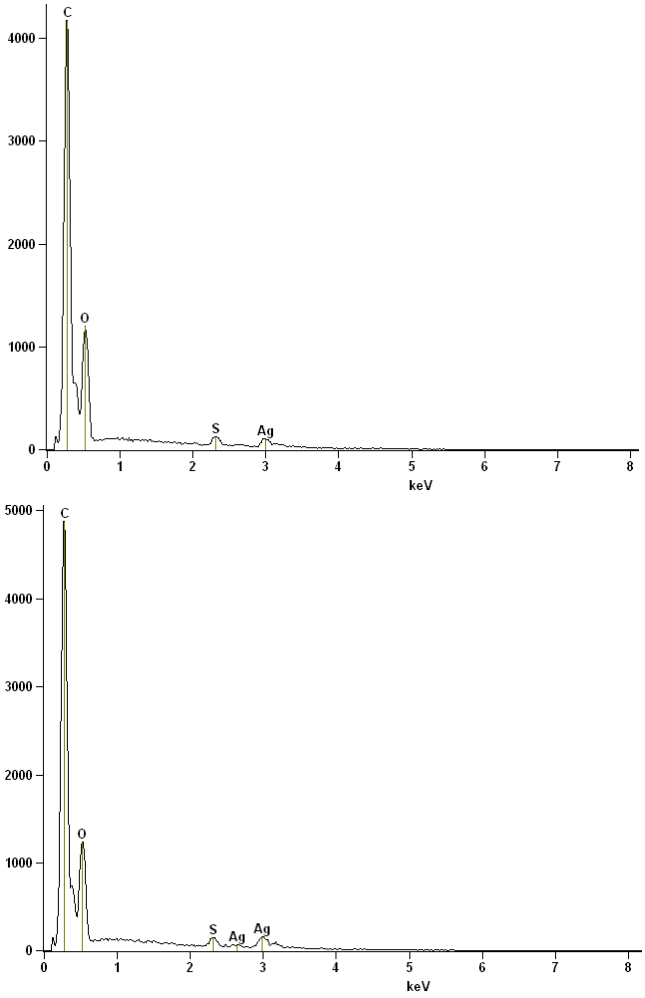

Figure 9: FEGSEM-EDS analysis for of the non–irradiated F1 (a), N5-b (b) and N5-w(c) sample, Acc. Voltage 6.0kV

Table 3: FEGSEM-EDS semi-quantitative results for F1, N5-b and N5-w samples

Element Line	Net Counts	Weight %	Atom %
Semi-quantitative Results for: F1 sample			
C K	24572	52.52	70.53
O K	9132	21.70	21.87
Al K	1169	1.76	1.05
P K	2849	7.00	3.64
S K	334	1.01	0.51
Ag L	1607	16.01	2.39
Total		100.00	100.00
Semi-quantitative Results for: N5-b sample			
C K	32799	58.36	77.70
O K	6778	17.58	17.57
S K	1103	3.31	1.65
Ag L	2062	20.75	3.08
Total		100.00	100.00
Semi-quantitative Results for: N5-w sample			
C K	38582	54.96	77.82
O K	7128	15.35	16.31
S K	1322	3.18	1.69
Ag L	3298	26.51	4.18
Total		100.00	100.00

b. Selected points individual semi-quantitative analyses

When the micrographs were analyzed, different kind of intensities and variations of white and black contrast can be associated with specific elements or with impurities and superficial contamination. For further investigation, different spots were analyzed to clarify their composition and the results of F1 are shown in Figure 10. White spots in the image are directly associated with silver. For N5 samples was found dust particles around the white spots on the films (silicon), however silver (Ag) is also present because in most of the films, Ag is located inside the polymer labels, as expected from the layered structure of the film.

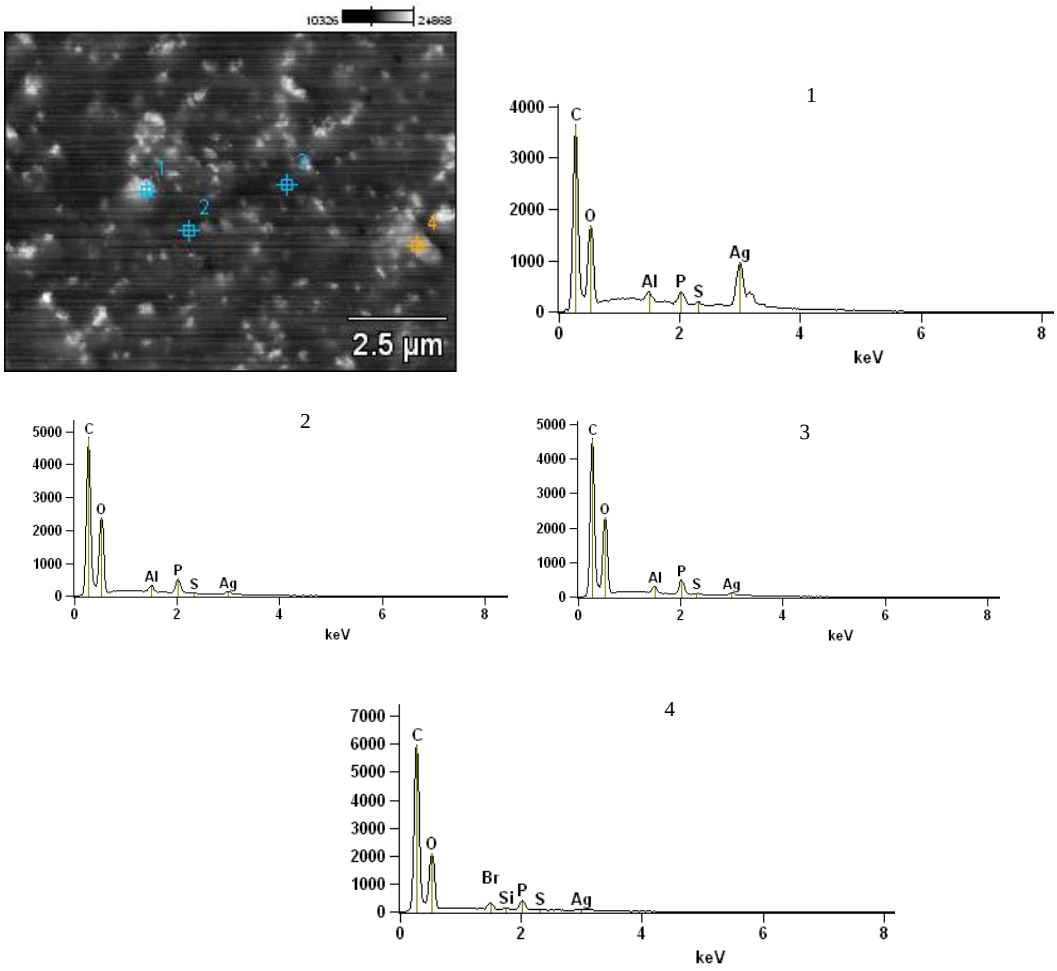

Weight %

	C-K	*O-K*	*Al-K*	*Si-K*	*P-K*	*S-K*	*Br-L*	*Ag-L*
F1_pt1	19.92	13.05	0.99		2.56	0.87		62.60
F1_pt2	51.61	26.40	1.72		7.30	0.87		12.11
F1_pt3	53.50	26.26	1.73		7.84	0.87		9.81
F1_pt4	60.42	19.87		0.57	4.89	1.32	3.92	9.02

Atom %

	C-K	*O-K*	*Al-K*	*Si-K*	*P-K*	*S-K*	*Br-L*	*Ag-L*
F1_pt1	51.81	25.49	1.14		2.59	0.85		18.13
F1_pt2	67.29	25.84	1.00		3.69	0.42		1.76
F1_pt3	68.21	25.13	0.98		3.87	0.42		1.39
F1_pt4	75.94	18.75		0.31	2.38	0.62	0.74	1.26

Figure 10: FEGSEM-EDS four (4) points semi-quantitative individual analysis for F1 sample.

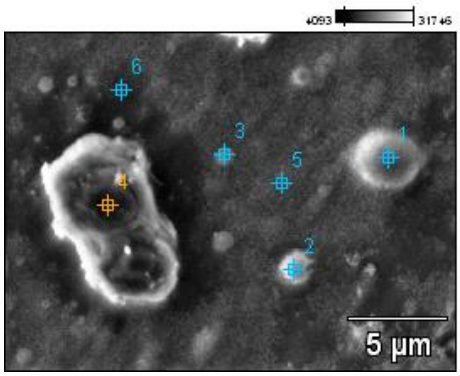
4093
317 46
6
3
1
5
4
2
5 µm

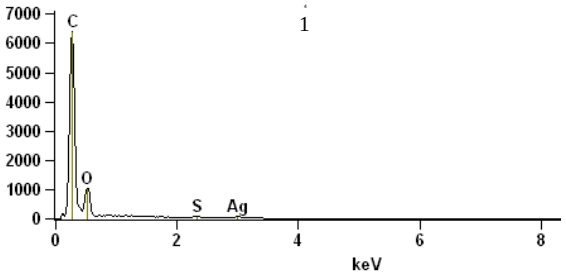
1
C
O
S
Ag
keV

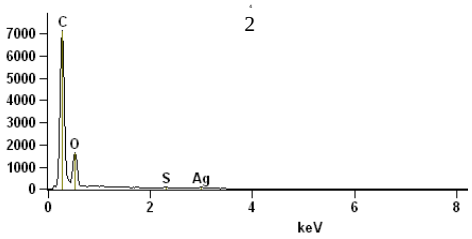
2
C
O
S
Ag
keV

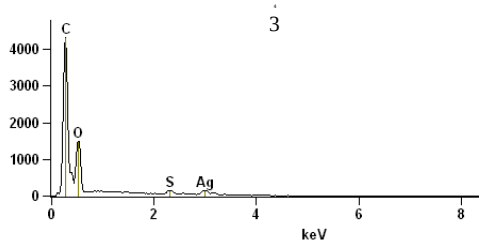
3
C
O
S
Ag
keV

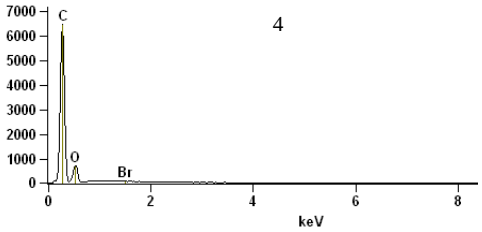
4
C
O
Br
keV

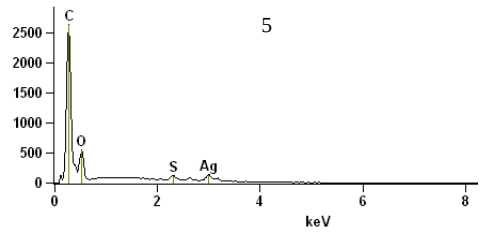
5
C
O
S
Ag
keV

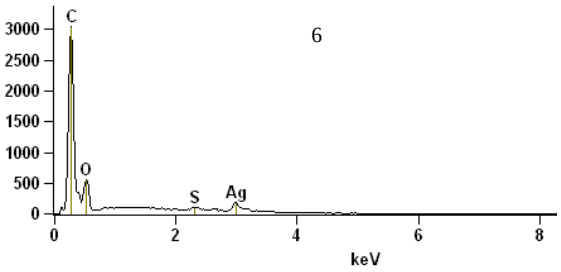
6
C
O
S
Ag
keV

	Weight %				
	C-K	***O-K***	***S-K***	***Br-L***	***Ag-L***
N5-b_pt1	74.18	14.46	1.79		9.57
N5-b_pt2	71.41	19.74	1.22		7.62
N5-b_pt3	51.41	20.78	3.17		24.64
N5-b_pt4	86.31	12.85		0.85	
N5-b_pt5	54.82	10.21	5.25		29.73
N5-b_pt6	48.94	9.69	3.31		38.07
	Atom %				
	C-K	***O-K***	***S-K***	***Br-L***	***Ag-L***
N5-b_pt1	85.49	12.51	0.77		1.23
N5-b_pt2	81.58	16.93	0.52		0.97
N5-b_pt3	72.46	21.99	1.67		3.87
N5-b_pt4	89.83	10.04		0.13	
N5-b_pt5	80.90	11.31	2.90		4.89
N5-b_pt6	79.33	11.79	2.01		6.87

Figure 11: FEGSEM-EDS six (6) points semi-quantitative individual analysis for N5-b sample.

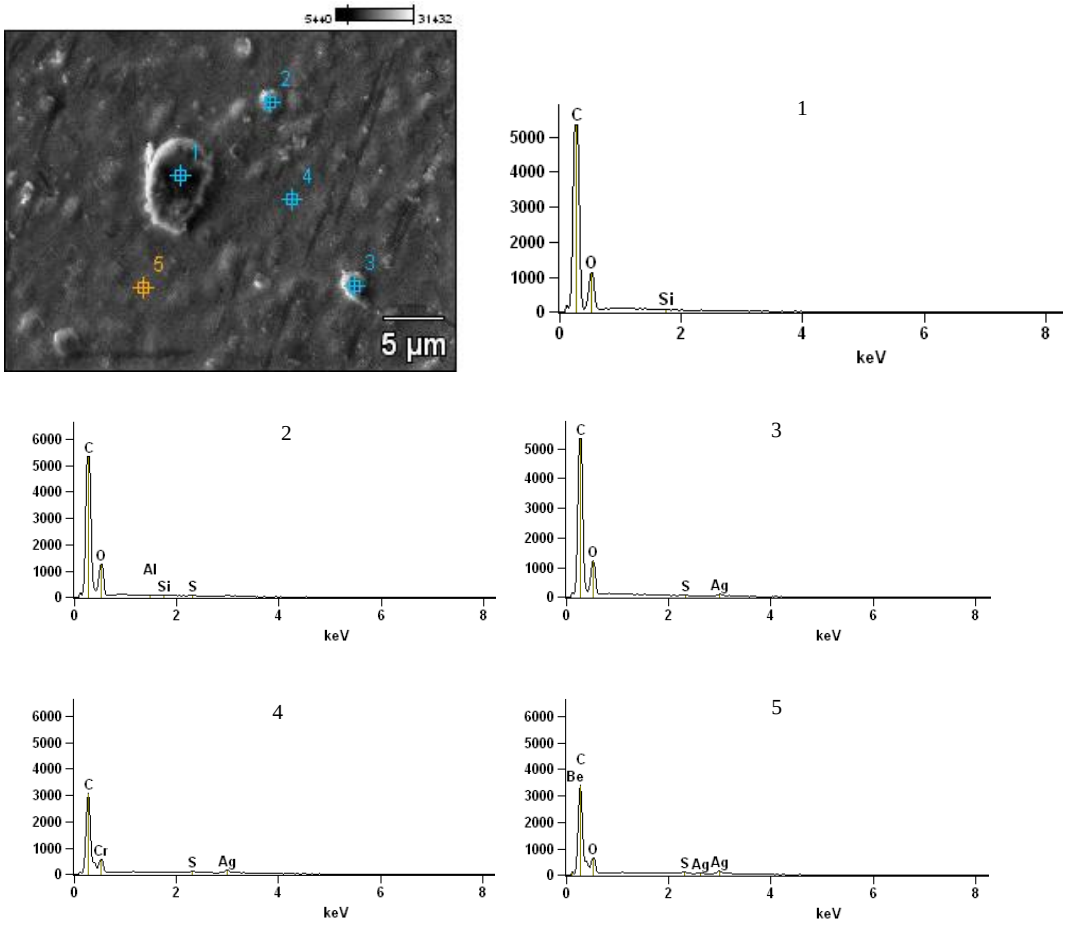

Weight %

	Be-K	*C-K*	*O-K*	*Al-K*	*Si-K*	*S-K*	*Cr-L*	*Ag-L*
N5-w_pt1		82.90	16.81		0.29			
N5-w_pt2		81.57	16.75	0.26	0.29	1.13		
N5-w_pt3		71.11	17.00			1.14		10.74
N5-w_pt4		41.36				3.48	32.77	22.39
N5-w_pt5	14.18	44.29	10.80			4.10		26.64

Atom %

	Be-K	*C-K*	*O-K*	*Al-K*	*Si-K*	*S-K*	*Cr-L*	*Ag-L*
N5-w_pt1		86.67	13.20		0.13			
N5-w_pt2		86.04	13.26	0.12	0.13	0.45		
N5-w_pt3		83.17	14.93			0.50		1.40
N5-w_pt4		78.44				2.47	14.36	4.73
N5-w_pt5	24.93	58.44	10.69			2.03		3.91

Figure 12: FEGSEM-EDS five (05) points semi-quantitative individual analysis for N5-w sample.

4. CONCLUSIONS

FTIR-ATR spectroscopy analysis characterized photographic and cinematographic samples with cellulose acetate base, gelatin emulsion and triphenyl phosphate. The UV-VIS spectra revealed no significant changes for irradiated samples until 50kGy. Electron microscopy revealed presence and a good distribution of silver in all samples. The microscopy images of the non-irradiated and 10 kGy irradiated samples did not show significant differences in the topographic morphology of the films. EDS spectra confirmed the composition of photographic and cinematographic films. The results obtained corroborate the studies of the application of gamma radiation to preserve materials of cellulosic origin. Hence, the present study demonstrated that the gamma radiation applied to photographic and cinematographic films of cellulose acetate support for fungi disinfection can be achieved safety applying dose between 6 kGy to 15kGy with no significant change or modification of main properties of the constitutive materials.

ACKNOWLEDGMENTS

The authors are grateful for financial support from the International Agency of Atomic Energy - IAEA.

REFERENCES

1. M. Edge, N. S. Allen, T. S. Jewitt, “Fundamental Aspects of the Degradation of Cellulose Triacetate Base Cinematograph Film,” *Polymer Degradation and Stability*, **25**, pp.345-362 (1989).

2. T. N. Blanton, J. A. Kaduk, Q. Johnson, “X-ray diffraction characterization of a distorted Debye–Scherrer film strip – the effect of deacetylation on cellulose triacetate and an improved structural model for cellulose II,” *Powder Diffraction*, **29(2)**, pp.108-112 (2014).
3. IAEA, Directory of Gamma Processing Facilities in Member States, IAEA-DGPF, Vienna, 2004.
4. IAEA, Guidelines for Industrial Radiation Sterilization of Disposable Medical Products (Cobalt -60 Gamma Irradiation). IAEA-TECDOC-539, Vienna, 1990.
5. G. Magaudda, “The recovery of biodeteriorated books and archive documents through gamma radiation: some considerations on the results achieved”, *Journal of Cultural Heritage*, **5**, pp. 113-118 (2004).
6. M.C. Area, A.M. Calvo, F.E. Felissia, A. Docters, M.V. Miranda, “Influence of dose and dose rate on the physical properties of commercial papers commonly used in libraries and archives”, *Radiation Physics and Chemistry*, **96**, pp. 217-222 (2014)
7. C. C. Ponta, “Irradiation Conservation of Cultural Heritage”, *Nuclear Physics News*, **18**:1, pp. 22-24 (2008).
8. IAEA, Radiation Safety of Gamma, Electron and X Ray Irradiation Facilities, IAEA Safety Standards Series No. SS-G-8, Vienna, 2010.
9. W.A.P. Calvo, P. Rela, L.G.A. Silva, “A small size continuous run industrial gamma irradiator”, *Radiation Physics and Chemistry*, **71**, pp.561-563 (2004).
10. R.M. Brinston, D.G. Levesque, “Irradiation on a new scale: Introducing Brevion”, Emerging Applications of Radiation Processing, IAEA-TECDOC- 1386, IAEA, Vienna (2004) 162.
11. IAEA, Technical Reports Series No. 409, Dosimetry for Food Irradiation, Vienna, (2002).
12. P.S. Santos, P.A.S. Vasquez, “Two-Faces Stationary Irradiation Method and Dosimetric Considerations for Radiation Processing at the Multipurpose Gamma Irradiation Facility/ IPEN-CNEN.” International Nuclear Atlantic Conference - INAC 2015, São Paulo, 2015.
13. P.S. Santos, P.A.S. Vasquez, “Effects of the Interruption of the Irradiation Process on PMMA Harwell Industry Dosimetry System”. International Nuclear Atlantic Conference - INAC 2015. São Paulo. 2015.
14. Y. Kodama, O. Jr. Rodrigues, R. H. L. Garcia, P.S. Santos, P.A.S. Vasquez. “Study of Free Radicals in Gamma Irradiated Cellulose of Cultural Heritage Materials Using Electron Paramagnetic Resonance.” *Radiation Physics and Chemistry*, 124, 2016. 169-173.
15. IAEA Technical Cooperation Project Report – RER 8015 “Using Nuclear Techniques for the Characterization and Preservation of Cultural Heritage Artefacts in the European Region”; *Nuclear Techniques for Preservation of Cultural Heritage Artefacts*, Vienna. 2014.